

*DETERMINATION OF CHARGED PARTICLE MASS FROM SCATTERING AND RESIDUAL RANGE IN MULTIPLATE CLOUD CHAMBERS*

F. R. ARUTYUNYAN

Physics Institute, Academy of Sciences, Armenian S.S.R.

Submitted to JETP editor August 15, 1958

J. Exptl. Theoret. Phys. (U.S.S.R.) **36**, 985-991 (April, 1959)

The method of determining the mass of a charged particle from its scattering and residual range in multiplate cloud chambers is experimentally checked by using it to determine the masses of protons,  $\mu$  and  $\pi$  mesons identified independently (from momentum-range data). The proton,  $\mu$ - and  $\pi$ -meson masses derived from the corresponding multiple Coulomb scattering curves are in good agreement with the correct values.

### 1. INTRODUCTION

A method of determining the mass of a charged particle from its scattering and residual range in multiplate cloud chambers has been proposed and described by Annis et al.<sup>1</sup> The present work is an experimental test and study of the possibilities of this method by using it to determine the masses of protons,  $\mu$  and  $\pi$  mesons which had been previously identified by an independent technique. Our preliminary data have already been published.<sup>2</sup>

When a charged particle is stopped inside a cloud chamber after being scattered in several plates a mean value for the experimental scattering angle can be computed. This mean angle can also be calculated from the theoretical distribution of multiple Coulomb scattering angles. The mean scattering angle and the rms scattering angle are the most frequently used characteristics of the scattering curve. However, instead of using the scattering angle  $\theta$  it is convenient to work with  $\eta = \theta R^\alpha$ ,<sup>1</sup> where  $R$  is the residual range of the particle and  $\alpha = 0.55$ , which is the same constant for all elements. The theoretical distribution of  $\eta$  and the angular distribution coincide except for the scale factor  $R^\alpha$ .

The mean and rms values of  $\eta$  given in reference 3 are

$$\langle \eta \rangle = A_1 (m_e / m)^{1-\alpha}, \quad (1)$$

$$\langle \eta^2 \rangle^{1/2} = A_2 (m_e / m)^{1-\alpha}, \quad (2)$$

where the coefficients  $A_1$  and  $A_2$  depend on the material and thickness of the scattering plates and the angular distribution function for multiple scattering. Ter-Mikaelyan<sup>3</sup> gives values of these coefficients for lead plates 7 and 4 mm thick taking finite nuclear size into account. Table I gives the values of  $A_1$  and  $A_2$  for the 7-mm plates which were calculated for finite nuclear size, for a point nucleus by Molière<sup>4</sup> and for the normal distribution of scattering angles.

We calculated  $A_1$  and  $A_2$  for copper plates only from the scattering curve for a point nucleus because in the case of copper finite nuclear dimensions are of negligible significance in the investigated momentum and angular ranges.

A sufficiently large number of observed angles for particles of the same type enables us to compute the mean and rms values of  $\eta$  and the particle mass  $m$  from (1) and (2).

### 2. EXPERIMENTAL RESULTS AND DISCUSSION

In order to test the given procedure for determining particle masses we used data on proton,  $\mu$ - and  $\pi$ -meson scattering in lead plates 7 and 4 mm thick and copper plates 5 and 2 mm thick, given in references 5 and 6, respectively. We also used data on  $\mu$ -meson scattering in 4-mm copper plates which have been obtained by Kirillov-Ugryumov et al.<sup>7</sup>

For our purposes we selected particles which traversed at least four plates of the total number

TABLE I

A	For finite model of nucleus <sup>3</sup>				For point model of nucleus	Normal distribution of scattering angles
	$\beta=0.50$	0.61	0.7825	0.8554		
$A_1$	520	532	550	561	611	566
$A_2$	655	672	694	711	776	708

TABLE II

n	Plate material	Type of particle		
		Protons	$\mu$ mesons	$\pi$ mesons
3-6	Pb	1500	465	169
	Cu	145	546	103

of 7 plates in the cloud chamber. Table II gives the total of selected protons,  $\mu$  and  $\pi$  mesons. The value of  $\eta$  was determined from the scattering angle and residual range for each scattering event individually. The values for each type of particle were grouped, and  $\langle \eta \rangle_{\text{exp}}$  and  $\langle \eta^2 \rangle_{\text{exp}}^{1/2}$  were calculated separately for protons,  $\mu$  and  $\pi$  mesons, after which (1) and (2) were used to determine the masses.

Certain features of the experiment strongly enhance the theoretical values of  $A_1$  and  $A_2$  which are given in Table I. For example, when the experimental geometry is taken into account (different angles are registered with different probabilities for scattering in the volume bounded by the instrument) we obtain an increased expectation number for large-angle scattering and thus derive larger values of  $A_1$  and  $A_2$ . We have given a detailed analysis of all these corrections in an earlier communication<sup>6</sup> and now regard these improved values of  $A_1$  and  $A_2$  as the computed values. For example, for the scattering curve taking finite nuclear size into account with 7-mm lead plates the computed values for  $\mu$  mesons are  $A_1 = 593$  and  $A_2 = 766$ , while for

a point nucleus they are  $A_1 = 665$  and  $A_2 = 849$ . The computed values of  $A_1$  and  $A_2$  for protons,  $\mu$  and  $\pi$  mesons differ because the corrections vary with the type of particle.

Table III gives the proton,  $\mu$ - and  $\pi$ -meson masses obtained in experiments with lead and copper plates separately. The  $\mu$ - and  $\pi$ -meson masses calculated by two methods (using  $\langle \eta \rangle$  and  $\langle \eta^2 \rangle^{1/2}$ ), from the scattering curve, taking finite nuclear size into account (for lead plates) and for a point nucleus (for copper plates), are in good agreement with the true masses. The  $\mu$ - and  $\pi$ -meson masses calculated from the scattering curve for a point nucleus in the case of lead plates are much too high and are incompatible with the masses calculated from the scattering curve for a finite nucleus.

We note that when we calculate the  $\mu$ - and  $\pi$ -meson masses from uncorrected values of  $A_1$  and  $A_2$  (Table I) the masses calculated from the corresponding curves are much too low (for example,  $(157 \pm 5)m_e$  for the  $\mu$  meson).

The proton mass calculated from the scattering curve for a finite nucleus when lead plates are used is only  $0.6 \pm 0.015$  of the correct mass by the  $\langle \eta^2 \rangle^{1/2}$  method and only 0.734 of the correct mass by the  $\langle \eta \rangle$  method. The calculations for a point nucleus gives a value which is close to the correct proton mass but still a little smaller.

In reference 5, where we presented our results on proton scattering, we showed that the

TABLE III

Particles	Method	Theory*	Lead plates 7 and 4 mm thick		Copper plates 5.4 and 2 mm thick	
			No. of scattering events, N	Mass, $m_e$	No. of scattering events, N	Mass, $m_e$
$\mu$ -mesons	$\langle \eta^2 \rangle^{1/2}$	1	2337	201 $\pm$ 7	—	—
		2	2337	267 $\pm$ 9	2740	210 $\pm$ 6
	$\langle \eta \rangle$	1	2337	211	27	—
		2	2337	262	2740	223
$\pi$ -mesons	$\langle \eta^2 \rangle^{1/2}$	1	818	286 $\pm$ 16	—	—
		2	818	386 $\pm$ 21	528	287 $\pm$ 19
	$\langle \eta \rangle$	1	818	289	—	—
		2	818	363	528	294
Protons	$\langle \eta^2 \rangle^{1/2}$	1	6187	1106 $\pm$ 22	580	1760 $\pm$ 115
		1'	6177	1243 $\pm$ 25		
		2	6187	1675 $\pm$ 34		
		2'	6177	1843 $\pm$ 37		
	$\langle \eta \rangle$	1	6187	1352	580	1805
		1'	6177	1425		
		2	6187	1770		
		2'	6177	1855		

\*1 - from the scattering curve for a finite nucleus, 2 - from the scattering curve for a point nucleus.

experimentally observed proton scattering-angle distribution is in good agreement with the multiple Coulomb scattering curve for a point nucleus. This results from the combined effects of the finite nuclear size and elastic nuclear scattering. Finite nuclear size and diffraction scattering are two mutually compensating factors, as a result of which the experimental scattering-angle distribution for protons can be well represented by the Coulomb scattering curve for a point nucleus. At large angles the experimental values lie above the Coulomb scattering curve for a point nucleus. When we cut off large scattering angles, which result from nuclear scattering, the proton mass can be calculated from the values of  $A_1$  and  $A_2$  computed from the Coulomb scattering curve for a point nucleus, since we do not possess values of  $A_1$  and  $A_2$  which take nuclear scattering into account.

The proton mass obtained, after the large-angle cutoff ( $\theta \geq 30^\circ$ ), from the scattering curve for a point nucleus is in excellent agreement with the correct value. When finite nuclear size is taken into account the proton mass is smaller than the correct value (these mass values are indicated by  $2'$  and  $1'$  in Table III). Table III also gives the proton mass calculated for copper plates for a point nucleus, which are in good agreement with the correct mass within the limits of statistical error.

We have published our results on  $\pi$ -meson scattering in reference 6. Diffraction scattering of  $\pi$ -mesons also occurs but affects the multiple-scattering part of the curve only slightly and the experimental angular distribution for  $\pi$ -mesons is in good agreement with the multiple Coulomb scattering curve for a finite nucleus. Diffraction scattering of  $\pi$ -mesons occurs only at large angles. The  $\pi$ -meson mass given in Table III was calculated from the scattering curve for a finite nucleus neglecting large angles.

In determining the masses of nuclear-active particles from scattering and residual range we therefore first exclude large angles, which are associated with nuclear scattering, and then calculate the masses of the particles from their scattering curves.

When the number of scattering events  $n$  is small, which occurs for a single stopping particle, the data must be treated more rigorously. To obtain a better estimate of the particle mass  $m$  we must know the distribution of  $\eta_2$ , the rms of  $\eta$ . Olbert<sup>8</sup> has obtained a formula for the distribution of  $\eta_2$ , from which normal angular distribution it follows that

$$\eta_{2 \text{ most prob}} = \left(\frac{n-1}{n}\right)^{1/2} \rho, \quad (3)$$

where

$$\rho = A_2 (m_e/m)^{1-\alpha} \quad (4)$$

and  $A_2$  is taken for the normal approximation. But since  $\eta_{2 \text{ most prob}}$  depends on  $\rho$  it is evident that for a mixture of particles with different  $\rho$  (different masses) the resultant distribution may consist of distinct parts. However, since  $\eta_{2 \text{ most prob}}$  depends only on the number  $n$  of the scattering events and this number is not the same for different trajectories, for each proton,  $\mu$ - and  $\pi$ -meson trajectory the quantity

$$\xi = \left(\frac{n}{n-1}\right)^{1/2} \eta_2 = \left(\frac{1}{n-1} \sum_{i=1}^n \eta_i^2\right)^{1/2}, \quad (5)$$

was set up separately, the most probable value of which depends only on  $\rho$  ( $\xi_{\text{most prob}} = \rho$ ).

We can thus separate particles of different masses by means of the distribution function of  $\xi$ :<sup>1</sup>

$$G_n(\xi, \rho) d\xi = \left(\frac{n-1}{2\rho^2}\right)^{1/2} F_n \left[\left(\frac{n-1}{2\rho^2}\right)^{1/2} \xi\right] d\xi, \quad (6)$$

where

$$F_n(\chi) d\chi = (2/\Gamma(n/2)) \chi^{n-1} \exp(-\chi^2) d\chi$$

is the  $\chi^2$  distribution for  $n$  degrees of freedom. The maximum of this functions corresponds to the most probable value of the mass  $m$ .

Statistical errors of the masses are calculated from the formulas in reference 1. The average number of scatterings on each trajectory is  $\bar{n} = 4$  for protons and  $\bar{n} = 5$  for mesons.

The experimental distributions of  $\xi$  for protons,  $\mu$ - and  $\pi$ -mesons and the corresponding theoretical curves of  $G_n(\xi, \rho)$  with lead plates inside the chamber are given in Fig. 1a. Fig. 1b gives the distributions for lead and copper plates combined. The horizontal axis represents values of  $\nu_\mu = \xi/\rho_\mu$ , where  $\rho_\mu$  is the value of  $\rho$  for  $\mu$ -mesons calculated from (4).

The angular distribution for multiple Coulomb scattering of  $\mu$  and  $\pi$  mesons in the given momentum range for the case of a finite nucleus and lead plates is well approximated by a normal distribution curve.<sup>3</sup> Fig. 1 shows that the experimental and theoretical values for  $\mu$  and  $\pi$  mesons are in good agreement.

For protons there is a large discrepancy between the experimental distribution of  $\xi$  and the theoretical curve  $G_n(\xi, \rho)$  (Fig. 1a and b) which shows that the function  $G_n(\xi, \rho)$  calculated for a normal distribution of scattering angles cannot be used for comparison with the actual non-

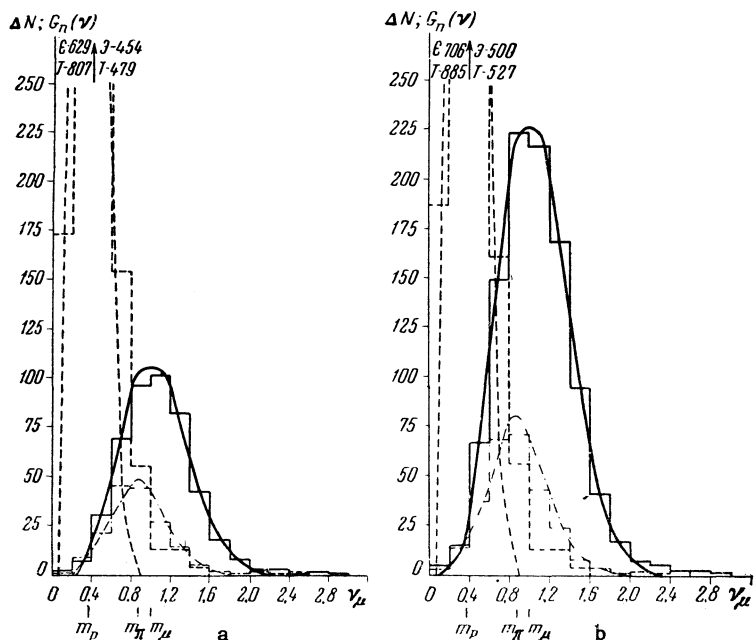


FIG. 1. Distribution of  $\xi$  for protons and mesons and corresponding theoretical curves  $G_n(\xi, \rho)$ : a – for lead plates and b – for lead and copper plates combined, with  $n = 3$  to 6. Protons – dashed lines;  $\mu$  and  $\pi$  mesons together – solid lines;  $\pi$  mesons separately – dot-dash lines. E and T – experimental and theoretical values of the ordinates instead of their graphical representation.

TABLE IV

n	Material	Type of particle		
		Protons	$\mu$ mesons	$\pi$ mesons
20–25	Pb	300	93	34
	Cu	29	109	21
40–50	Pb	150	47	17
	Cu	15	55	11

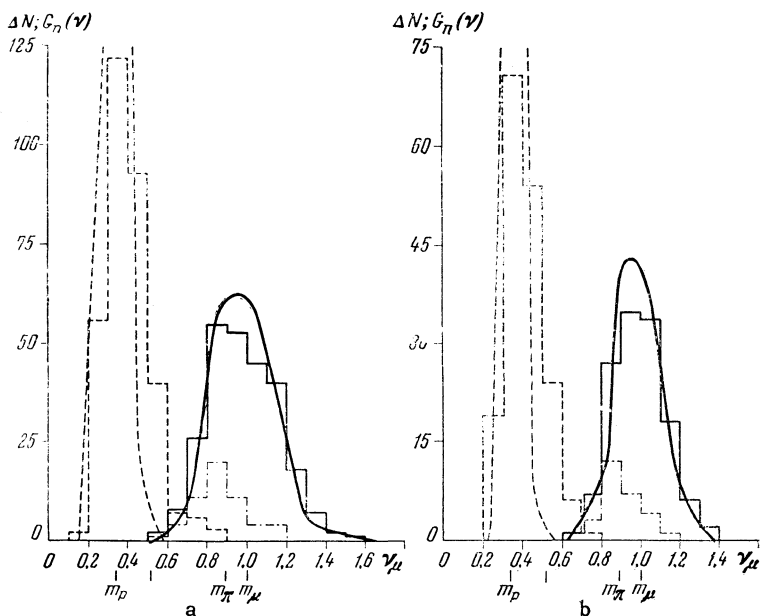


FIG. 2. Distribution of  $\xi$  for protons and mesons and corresponding theoretical curves  $G_n(\xi, \rho)$ : a – for  $n = 20$  to 25; b –  $n = 40$  to 45; for lead and copper plates combined. Protons – dashed lines;  $\mu$  and  $\pi$  mesons combined – solid lines;  $\pi$  mesons separately – dot-dash lines.

normal distribution of proton scattering angles. Annis et al<sup>1</sup> have plotted a similar distribution for protons and  $\pi$ -mesons, assuming that all values of  $\xi$  to the left of the intersection of  $G_n(\xi, \rho)$  curves can be assigned to protons and all values to the right to  $\pi$  mesons. It is clear from Fig. 1 that the area to the right of the intersection of the  $G_n(\xi, \rho)$  curves for protons and mesons contains a considerable number of  $\xi$  values for protons; by cutting these off the authors of reference 1 would necessarily obtain an excessively large proton mass. Moreover, by using values of  $A_1$  and  $A_2$  calculated for scattering from a finite nucleus (which was not done quite correctly, and we have already shown that such values cannot be used to determine the proton mass), they obtained

a proton mass which approximates the correct mass more or less. On the other hand, by cutting off small values of  $\xi$  for  $\pi$  mesons the mass obtained for these particles was too low. As the number of scatterings along an individual trajectory increases the mass determination becomes more accurate. In order to determine the number  $n$  of scattering events along a single trajectory which would permit complete separation of protons and mesons, the values of  $\eta$  for the same type of particle were put into groups of 20 – 25 at 40 – 50 in succession (without any selection) and  $\xi$  was obtained for each of these groups separately; the numbers of these groups are given in Table IV. The experimental distributions of  $\xi$  for  $n =$

20 — 25 and  $n = 40 - 50$  and the corresponding theoretical  $G(\xi, \rho)$  curves for protons and mesons are shown in Fig. 2a and b from data for lead and copper plates combined; the  $\xi$  distributions for  $\mu$  and  $\pi$  mesons are here combined.

Protons and mesons are separated practically completely with  $n = 20 - 25$ .

In conclusion the author wishes to thank Professor A. I. Alikhanyan, M. L. Ter-Mikaelyan and M. I. Daŕon for their interest and participation in a discussion of the results.

---

<sup>1</sup>Annis, Bridge, and Olbert, Phys. Rev. **89**, 1216 (1953).

<sup>2</sup>Arutyunyan, Daŕon, and Ter-Saakyan, Izv. Akad. Nauk Armenian SSR **11**, 71 (1958).

<sup>3</sup>M. L. Ter-Mikaelyan, J. Exptl. Theoret.

Phys. (U.S.S.R.) **36**, 253 (1959). Soviet Phys. JETP **9**, 171 (1959).

<sup>4</sup>G. Molière, Z. Naturforsch. **3a**, 78 (1948); **2a**, 133 (1947).

<sup>5</sup>F. R. Arutyunyan, J. Exptl. Theoret. Phys. (U.S.S.R.) **34**, 800 (1958), Soviet Phys. JETP **7**, 552 (1958).

<sup>6</sup>A. I. Alikhanyan and F. R. Arutyunyan, J. Exptl. Theoret. Phys. (U.S.S.R.) **36**, 32 (1959). Soviet Phys. JETP **9**, 23 (1959).

<sup>7</sup>Kirillov-Urgyumov, Dolgosheŕn, Moskvichev and Morozova, J. Exptl. Theoret. Phys. (U.S.S.R.) **36**, 416 (1959), Soviet Phys. JETP **9**, 290 (1959).

<sup>8</sup>S. Olbert, Phys. Rev. **37**, 319 (1952).

Translated by I. Emin

196